Dinamika Teknik Mesin 16(1) (2026) 23-34

Dinamika Teknik Mesin
Jurnal Keilmuan dan Terapan Teknik Mesin
http://dinamika.unram.ac.id/index.php/DTM/index

Topology optimization of dji f450 drone arm using finite element analysis and additive manufacturing

Andreas[1*], M.A. Choiron [2], I.M.G. Karohika[1], A. Ghurri [1]
[1]Mechanical Engineering Department, Engineering Faculty, Udayana University, Jl. Raya Kampus UNUD, Jimbaran, South Kuta, Badung Regency, Bali 80361, Indonesia.
[2]Mechanical Engineering Department, Engineering Faculty, Brawijaya University, Jl. Veteran, Ketawanggede, Lowokwaru District, Malang City, East Java 65145, Indonesia.
*Corresponding author: andreas.220553118@student.unud.ac.id

ARTICLE INFO

Article History:
Received 07-12-2025
Accepted 30-01-2026
Available online 01-04-2026

Keywords:
Drone arm
Topology optimization
Additive manufacturing
Static simulation
Energy efficiency

ABSTRACT

This study presents the design, topology optimization, additive manufacturing, and experimental validation of a DJI F450 drone arm to enhance structural efficiency and energy performance. The original arm, made of PA66-30GF, was replaced with PLA for 3D printing, and topology optimization was applied to reduce mass while maintaining stiffness. Static structural simulations under thrust and lateral loads showed that the optimized design (Design 2.0) significantly reduced maximum stress and deformation under vertical load, while remaining within safe limits under lateral load. Experimental deformation tests validated the simulation results, with deviations of 0.64–3.89%. Flight tests demonstrated that Design 2.0 reduced battery consumption by 14.3% during 5-minute hovering, extending flight time by approximately 50 seconds. The study confirms that combining topology optimization with additive manufacturing can produce lightweight, high-performance drone components that improve both structural integrity and operational efficiency.

Dinamika Teknik Mesin, Vol. 16, No. 1, April 20256 ***p. ISSN: 2088-088X, e. ISSN:*** **2502-1729**

1. INTRODUCTION

Unmanned Aerial Vehicles (UAVs), commonly known as drones, are pilotless aircraft controlled remotely via command systems. Over the past few decades, drone technology has evolved rapidly and has been widely adopted in various sectors, including surveillance, logistics, search and rescue, agriculture, meteorology, and creative industries such as photography and videography. Drones offer significant advantages such as time efficiency, energy savings, and reduced safety risks for operators in hazardous missions. These advantages have prompted many countries to pursue advancements in drone technology (Hossain, 2022).

As drone applications continue to expand, the demand for structurally efficient and lightweight designs is increasing. One of the main factors affecting drone performance and energy efficiency is structural mass. A lighter drone requires less thrust, enabling motors to operate at lower, more energy-efficient speeds (Thibbotuwawa et al., 2019; Abeywickrama et al., 2018). Therefore, optimizing the structural design is essential to achieve both enhanced flight performance and power efficiency.

https://doi.org/10.29303/dtm.v16i1.1218

To meet these challenges, design approaches must not only minimize structural mass but also retain mechanical integrity. One of the most effective methods is topology optimization, a mathematical approach that determines the optimal material distribution by removing regions that do not significantly support the load (Bay & Eryıldız, 2024; Karohika et al., 2024). To facilitate the implementation of such advanced design methods, engineering simulation software such as ANSYS, SolidWorks Simulation, Altair HyperWorks, and Autodesk Fusion 360 serve as essential tools in modern engineering design. These platforms support various stages of the design process, enabling engineers to conduct structural analysis, evaluate performance, and optimize components with greater efficiency, accuracy, and speed (Asif et al., 2024; Winangun et al., 2024; Bright et al., 2021).

However, even though topology optimization can generate highly efficient and lightweight designs, the optimized structures are often complex and difficult to manufacture using conventional methods. This limitation can be overcome by implementing Additive Manufacturing (AM), or 3D printing, which enables the direct fabrication of intricate structures from digital models (Al-Haddad et al., 2024; Ngo et al., 2018; MatWeb, 2025). AM is particularly well-suited for realizing complex topologically optimized geometries that traditional subtractive methods cannot produce efficiently.

A previous study by Michał Kowalik (2024) successfully applied topology optimization and generative design to the DJI F450 drone frame, achieving more than 10% mass reduction with a safety factor of above 1.5. In contrast, this study focuses specifically on the DJI F450 drone arm, aiming for a 30–40% mass reduction of the arm component while maintaining a safety factor above 4. The optimization process is conducted using ANSYS Workbench to achieve an efficient material distribution along the primary load paths. The optimized design is then fabricated using Additive Manufacturing (3D printing) with PLA material. Furthermore, experimental deformation tests are conducted to validate the simulation results, and flight experiments are performed to evaluate the impact of the optimized arm on the drone's energy efficiency.

This study provides several scientific contributions to the field of lightweight UAV structural design. First, it presents an integrated methodology combining topology optimization, finite element analysis, additive manufacturing, and experimental validation specifically applied to a drone arm component, which has received less attention compared to full-frame optimization. Second, this research demonstrates how structural mass reduction can be directly correlated with energy efficiency and flight endurance, providing quantitative experimental evidence linking structural optimization with operational performance.

In addition, the study offers practical insight into the manufacturability of topology-optimized UAV components using fused filament fabrication (FFF) with PLA material, including validation through deformation testing and real flight experiments. These findings contribute to the development of efficient, manufacturable, and lightweight UAV structures and provide a reference framework for future research on performance-oriented structural optimization in small unmanned aerial systems.

2. RESEARCH METHODS

2.1 Materials

The frame of the DJI F450 drone consists of two main materials. The arm section (drone arm) is made of PA66-30GF, a type of polyamide 66 (nylon) reinforced with 30% glass fiber, which provides high mechanical strength and thermal resistance. Meanwhile, the upper and bottom frame sections are made of Printed Circuit Board (PCB)-based material, which not only serves as the main mechanical support but also functions as a power and signal distribution path for the drone's electronic components.

For the optimization and fabrication stages, the upper and bottom frames retained their PCB-based material, while the drone arms were replaced with PLA (Polylactic Acid), a lightweight thermoplastic commonly used in additive manufacturing due to its good dimensional stability and ease of printing. The mechanical properties of each material used in the modeling process are presented in Table 1 (Soon et al., 2024; Zadravec et al., 2025; Ultimaker, 2022; Hanon et al., 2021).

Table 1. Mechanical properties of materials used in DJI F450 frame components

Material	Density	Young's modulus	Yield strength
PA66-30GF	1370 kg/m^3	7 Gpa	54.35 MPa
PCB	1900 kg/m^3	24 Gpa	130 MPa
PLA	1290 kg/ m^3	3250 Mpa	38 Mpa

The main structural components of the DJI F450 drone frame consist of six parts: one upper plate, one bottom plate, and four drone arms. This configuration forms the primary structural framework that supports the entire electronic and propulsion system. In its standard configuration, the DJI F450 is designed to withstand a total thrust force of up to 40 N (Kowalik, Śliwiński, & Papis, 2025), generated simultaneously by all four

https://doi.org/10.29303/dtm.v16i1.1218

motors. Figure 1 illustrates the overall design and geometric configuration of the DJI F450 drone frame (Aravind, 2025). Table 2 details the drone components and their mass.

Table 2 Components mass drone DJI F450

Components	Mass	Sum
Upper plate	0.031 kg	1
Bottom plate	0.057 kg	1
Drone Arm	0.064 kg	4
Total	0.334 kg	6

The research began with dimensional measurements of the original DJI F450 drone arm to obtain accurate geometric data. The data served as the foundation for developing the initial design, which later became the basis for topology optimization. The initial model features a right-triangular configuration connecting the upper frame, lower frame, and motor mount, effectively representing the structural load path that transmits the motor's thrust force to the center frame.

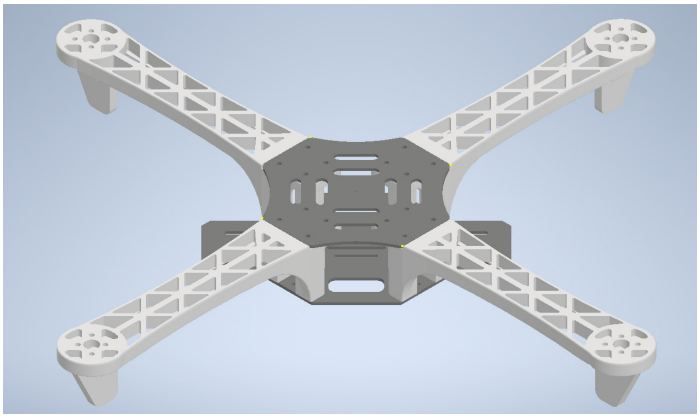

Figure 1. Original structural configuration of the DJI F450 quadcopter drone

Each motor mount was modeled as a cylindrical feature with a 30 mm diameter and 5 mm height—10 mm smaller than the original design—yet still sufficient to support the electric motors. The initial arm design is shown in Figure 2.

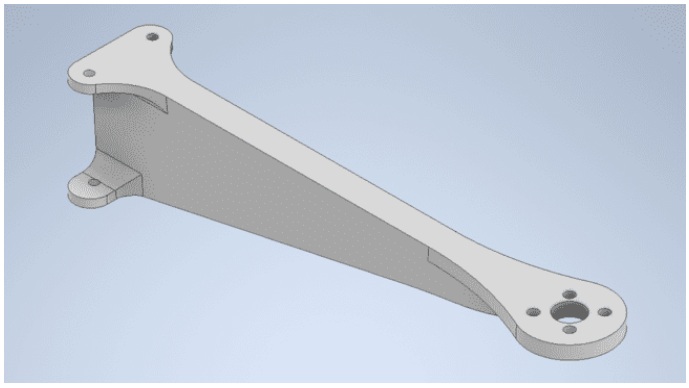

Figure 2. Initial design of drone arm

2.2 Static structural simulation

Static structure simulation was performed using ANSYS Workbench software to evaluate the mechanical response of the drone structure under thrust forces applied to each drone arm. The simulation parameters and boundary conditions are outlined as follows:

- Mesh element size: 0.002 m (2 mm), selected to balance computational accuracy and processing time.
- Support condition (Fixed Support): Applied to the bottom plate area, which is assumed to remain stationary during drone operation.

https://doi.org/10.29303/dtm.v16i1.1218

- Loading: A thrust load of 10 N was applied vertically upward to each motor mount. Additionally, a motor torque of τ_motor = 0.013 N·m was applied to each motor mount. The torque directions follow the standard quadrotor configuration, where two motors rotate clockwise (CW) and the other two rotate counterclockwise (CCW) (Darsin et al., 2025) .
- Observed variables: Von Mises stress, deformation, and Safety factor.

Figure 3 illustrates the boundary conditions and the direction of the applied loads used in the static structural simulation.

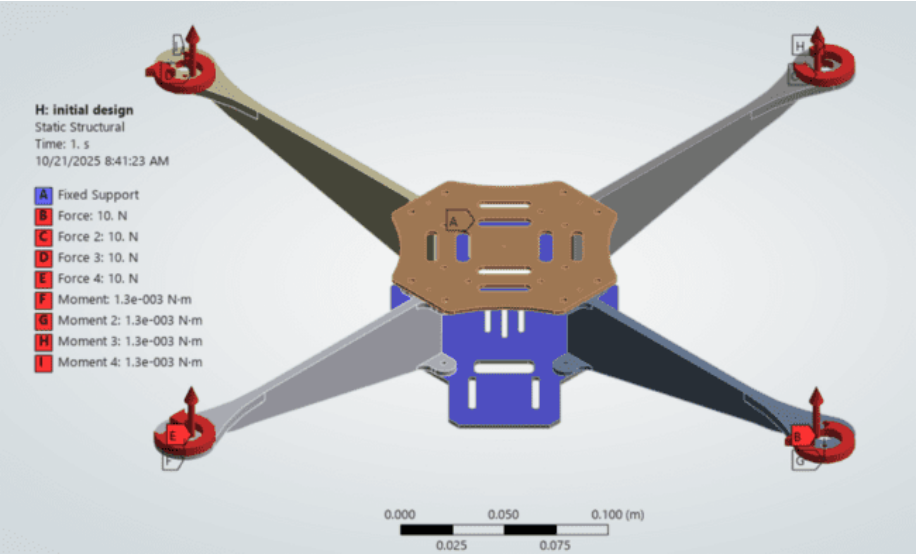

Figure 3. Free body diagram of the drone arm under Thrust load simulation

In the lateral load simulation, the following boundary conditions were applied:

- Fixed Support: Applied to the bolt areas connecting the drone arm to the main frame, replicating the physical constraints of the assembly.
- Loading: A lateral force of 5 N was applied at the motor mount, representing the side force acting on the arm during flight maneuvers.
- Observed Variables: Deformation and safety factor were measured to assess the structural response under lateral loading.

Figure 4 illustrates the boundary conditions and the direction of the applied loads used in the static structural simulation

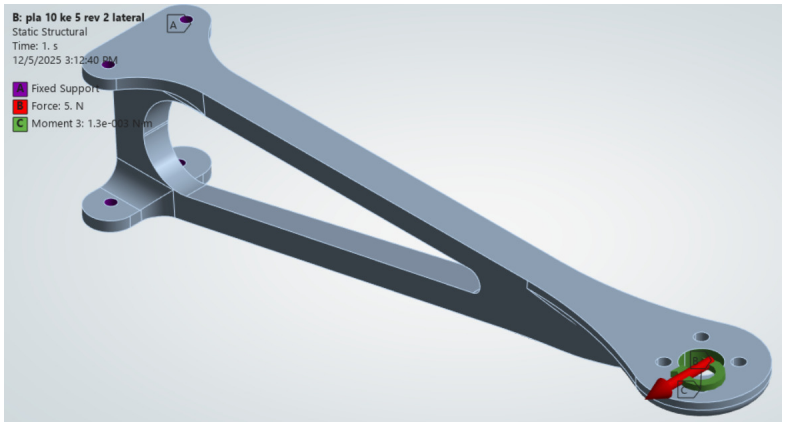

Figure 4. Free body diagram of the drone arm under lateral load simulation

https://doi.org/10.29303/dtm.v16i1.1218

2.3 Topology optimization dan 3D printing

Topology optimization was performed exclusively on the drone arm component using ANSYS Workbench, with the objective of achieving a lightweight yet stiff structure. The optimization parameters were set as follows:

- Objective: Minimization of compliance (to maximize stiffness)
- Response constraint: Mass ≤ 80% of the initial model mass
- Topology type: Mixable Density
- Manufacturing constraint: Extrusion along the Z-axis

The mass retention value of 80% was selected to achieve an optimal balance between structural weight reduction and mechanical performance. This constraint ensured that the optimized drone arm maintained a safety factor greater than 4 while still providing meaningful mass reduction.

The optimized model was fabricated using the Bambu Lab X1 Carbon 3D printer, capable of producing complex geometries with high precision. This additive manufacturing process enabled realization of the optimized arm design that would be difficult to manufacture conventionally. The printing parameters are summarized in Table 3.

Table 3. Print settings of Bambu Lab X1-carbon 3D printing.

Parameters	Value
Nozzle temperature	210 °c
Bed temperature	60 °c
Nozzle diameter	0.4 mm
Layer height	0.2mm
Printing speed	200 mm/s
Fan	On

2.4 Experimental

To verify the simulation results, an experimental deformation test was conducted on the final prototype (Design 2.0), which represents the topology-optimized and 3D-printed version of the DJI F450 drone arm. The objective of this test was to evaluate the actual deformation response under vertical and lateral loading conditions and to compare it with the numerical simulation results.

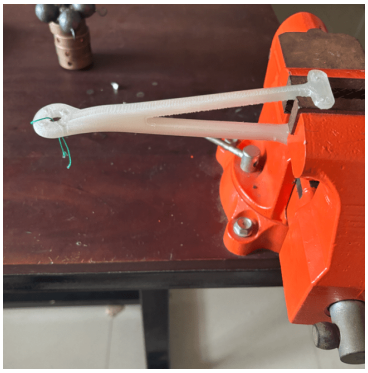

Figure 5. The experimental setup for vertical load

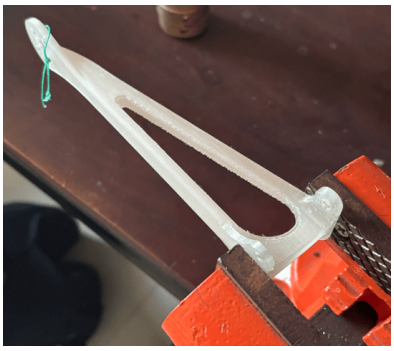

Figure 6. The experimental setup for lateral load

https://doi.org/10.29303/dtm.v16i1.1218

Figure 7. Applied load on the experiment setup

During the test, the specimen was firmly clamped using a bench vise, replicating the fixed boundary condition applied in the simulation. Controlled vertical and lateral loads were applied using calibrated weights, while the deformation was measured manually using a digital caliper with an accuracy of 0.01 mm. The measurement was reference points before and after loading, performed by comparing the distance between specific using the table surface beneath the specimen as a fixed reference plane. The difference between these two measurements represented the deformation experienced by the drone arm. Figures 5, 6 and 7 show the experimental setup and the applied loading configuration.

2.5 Flight test

To evaluate the operational performance of the optimized frame, the drone was assembled using the following components: DJI F450 frame, Li-Po 3S 3300 mAh battery, RCTIMER 880 KV brushless motors, Beatles 40A ESC with BEC, flight controller, and receiver. The flight test was carried out in Stabilize Mode under manual pilot control, conducted indoors to minimize wind disturbance. Each test consisted of a 5-minute hovering flight using two frame configurations: the Original Design and Design 2.0 (topology-optimized and 3D-printed version). During the flight, the pilot maintained a steady throttle position without abrupt inputs to keep the drone stable in hovering. Three flight trials were performed for each configuration to ensure repeatability. The measured parameters in this experiment were:

1. Final battery voltage (V) after the 5-minute hovering flight, measured for each of the three Li-Po cells in the 3S battery configuration.
2. Recharged electrical capacity (mAh), defined as the amount of electrical charge required to fully recharge the battery to its nominal full capacity after each flight test.

The recharged capacity was recorded using a Li-Po balance charger, which indicates the total milliampere-hour (mAh) input during the charging process. These parameters were used to evaluate and compare the energy consumption between the original and optimized drone arm configurations.

3. RESULTS AND DISCUSSION

The topology optimization results demonstrate that significant material removal occurred primarily in the midsection of the drone arm, where stress distribution was relatively low. In contrast, critical regions such as the motor mount, joint interfaces, and load transfer paths were preserved to maintain structural integrity. This material redistribution resulted in a structurally efficient design that maintains stiffness while reducing unnecessary mass.

The optimized arm exhibited approximately 53.1% mass reduction, decreasing from 64 grams in the original design to 30 grams in the final fabricated model. Despite this reduction, the optimized topology preserved the primary load paths, ensuring that stresses remained within safe limits and structural performance was maintained.

The generated topology produced an irregular organic geometry. Therefore, geometric refinement was required to ensure manufacturability using additive manufacturing while preserving the essential load-bearing structure. The final CAD model retained the optimized material distribution and was successfully prepared for 3D printing. Figure 8 shows the result of the topology optimization process and the final CAD design after topology optimization and geometric refinement.

https://doi.org/10.29303/dtm.v16i1.1218

a) b)

Figure 8. a) Topology optimization result, b) Final CAD design

These results indicate that topology optimization effectively improves structural efficiency by removing non-load-bearing material while maintaining mechanical performance, consistent with previous studies on lightweight UAV structural design (Zhu et al., 2018).

Static structural simulations were conducted on both the original and optimized drone arm (Design 2.0) to evaluate their mechanical performance under two primary loading conditions: propeller thrust load and lateral load. These loading scenarios represent the dominant forces experienced during hovering and minor lateral disturbances during flight.

Under propeller thrust loading, the optimized design demonstrated significantly improved structural performance compared to the original model. As shown in Table 4 and Figure 9, the maximum von Mises stress decreased substantially from 15.909 MPa in the original design to 3.01 MPa in Design 2.0. Similarly, the maximum deformation was reduced from 2.254 mm to 0.56 mm, while the safety factor increased from 8.17 to 15, indicating enhanced stiffness and structural reliability.

Table 4. Static structure simulation result under propeller thrust load

Design	Original	2.0
Maximum Von Mises Stress (MPa)	15.909	3.01
Maximum Deformation (mm)	2.254	0.56
Safety Factor	8.17	15

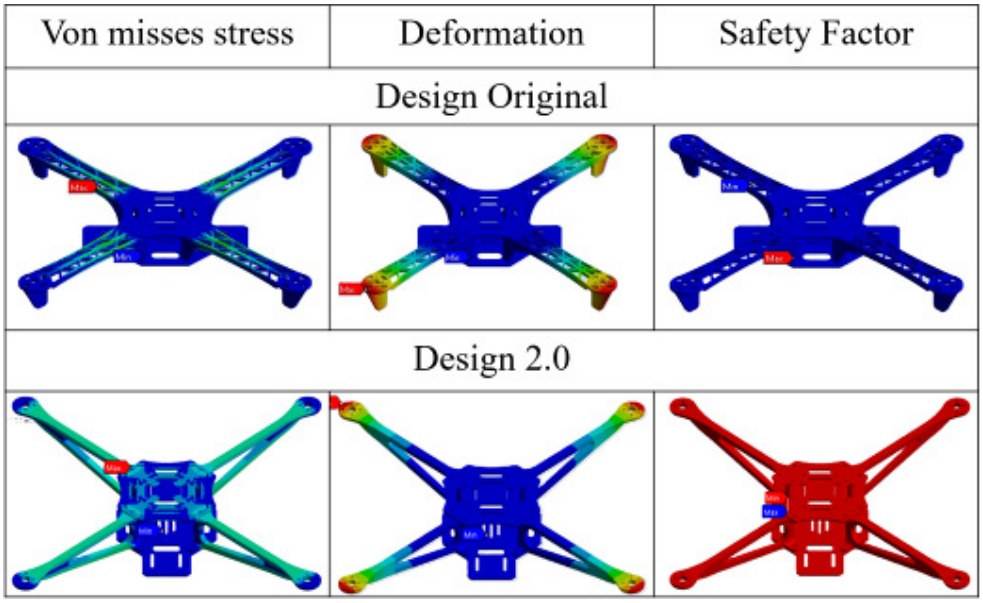

Figure 9. Stress, deformation, and safety factor distribution of Original and Design 2.0 under thrust load.

A notable difference can also be observed in the stress distribution patterns. In the original design, stress was highly concentrated at a specific region located in the midsection of the drone arm, forming a localized stress concentration. This condition is visible in Figure 9 through the stress contour color distribution. Such localized stress concentration may increase the potential risk of structural failure under continuous loading conditions.

https://doi.org/10.29303/dtm.v16i1.1218

In contrast, Design 2.0 exhibits a more uniform stress distribution along the arm structure. The stress contour visualization shows a more evenly distributed color pattern compared to the original design, indicating that the applied load is transferred more efficiently throughout the structure. This uniform stress distribution reduces peak stress concentration and improves structural durability. The improvement is attributed to the topology optimization process, which redistributes material along the primary load paths between the motor mount and frame connection while removing non-load-bearing regions. As a result, the optimized design achieves higher stiffness-to-weight efficiency under thrust loading.

Under lateral loading conditions, Design 2.0 exhibited higher deformation and a lower safety factor compared to the original design, as presented in Table 5 and Figure 10. The maximum deformation increased from 0.12 mm in the original design to 4 mm in the optimized design, while the safety factor decreased from 15 to 4.95. This behavior is expected because the topology optimization process primarily considered vertical thrust as the dominant loading scenario. Consequently, some material that previously contributed to lateral stiffness was reduced to achieve weight efficiency.

Table 5. Static structure simulation result under lateral load

Design	Original	2.0
Maximum Deformation (mm)	0.12	4
Safety Factor	15	4.95

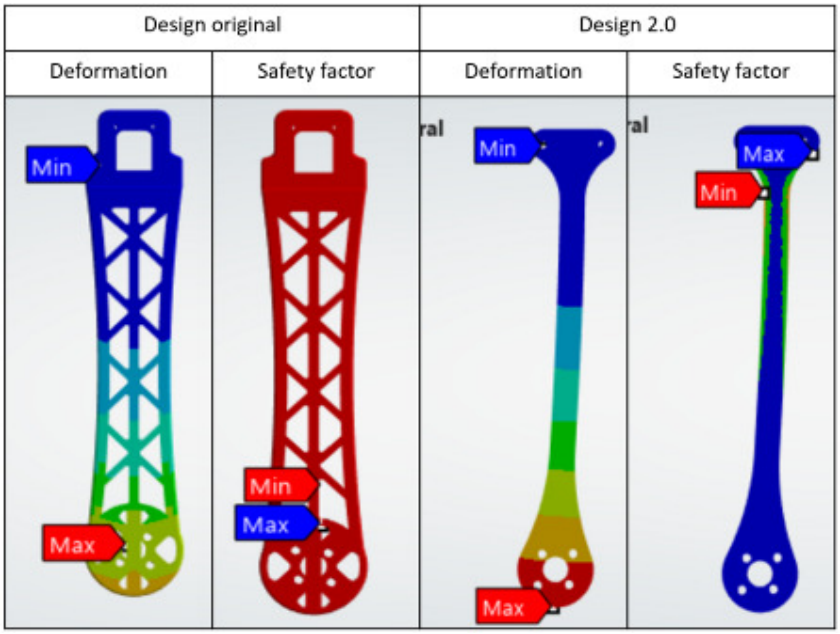

Figure 10. Stress, deformation, and safety factor distribution of design original and design 2.0 under lateral load.

Despite the reduction in lateral stiffness, the safety factor of Design 2.0 remains above 4, indicating that the structure is still within acceptable mechanical safety limits. In practical UAV operation, lateral loads during hovering are relatively small compared to vertical thrust generated by the propellers. Therefore, the optimized design maintains sufficient structural safety while achieving significant weight reduction.

Overall, the simulation results confirm that topology optimization successfully improves structural efficiency by enhancing stiffness-to-weight ratio under dominant thrust loading while maintaining acceptable performance under secondary lateral loading conditions.

The prototype was produced using the Bambu Lab X1 Carbon printer with PLA material, successfully realizing the complex geometry resulting from the topology optimization process. The printed prototype retained the essential structural characteristics of the digital model while achieving good surface quality and dimensional precision. A significant weight reduction was achieved through this process. The final mass of the fabricated optimized arm was 30 grams, compared to 64 grams for the original design, representing a 53.1% reduction in component weight. The use of PLA material combined with additive manufacturing further enabled efficient material usage by allowing internal voids and complex geometries to be produced without additional assembly.

The reduction in component mass contributes directly to improved overall drone performance. A lighter structural mass reduces the total take-off weight of the UAV, which in turn decreases the thrust required from the

https://doi.org/10.29303/dtm.v16i1.1218

propulsion system to maintain hovering. Lower thrust demand leads to reduced motor workload and lower electrical current consumption, thereby improving energy efficiency and potentially extending flight endurance. (Abeywickrama et al., 2018). At the same time, structural analysis results confirmed that the optimized arm maintains adequate strength and safety factors, ensuring that weight reduction does not compromise structural reliability. Figure 11 shows the final 3D-printed drone arm prototype (Design 2.0) .

Figure 11. 3D-Printed result of the drone arm

Experimental validation was conducted to verify the accuracy of the finite element simulation and to evaluate the actual mechanical behavior of the optimized drone arm under vertical (thrust) and lateral loading conditions. Incremental loads were applied to the fabricated drone arm while the resulting deformation was measured using a displacement measuring device. The experimental results were then compared with the corresponding numerical simulation outputs. Tables 6 and 7 summarize the simulation and experimental results, while Figures 12 and 13 present the comparative graphs.

Table 6. Simulation results

Thrust Load		Lateral Load	
Load (N)	Deformation (mm)	Load (N)	Deformation (mm)
5	0.2774	2	1.608
10	0.554	5	4.01
15	0.8324	8	6.411

Table 7. Experimental results

Thrust Load			Lateral Load		
Mass (g)	Load (N)	Deformation (mm)	Mass (g)	Load (N)	Deformation (mm)
517	5.0666	0.28	204	1.9992	1.59
1023	10.0254	0.56	518	5.0764	3.9
1536	15.0528	0.8	807	7.9086	6.37

Overall, the experimental results showed strong agreement with the simulation predictions under both loading conditions. As the applied load increased, both simulation and experimental data exhibited proportional increases in deformation, indicating elastic structural behavior within the tested load range. Under thrust loading, the deviation between simulation and experimental results ranged from approximately 0.93% to 3.89%, with an average deviation of about 1.97%. Meanwhile, under lateral loading, the deviation ranged from approximately 0.64% to 2.50%, with an average deviation of about 1.50%. The overall average deviation between simulation and experimental results was approximately 1.7%, which is well below the commonly accepted tolerance limit of 5% for structural validation studies (Shu et al., 2021). This close agreement confirms that the material properties, boundary conditions, and loading assumptions defined in the finite element model accurately represent the real structural behavior of the optimized drone arm.

https://doi.org/10.29303/dtm.v16i1.1218

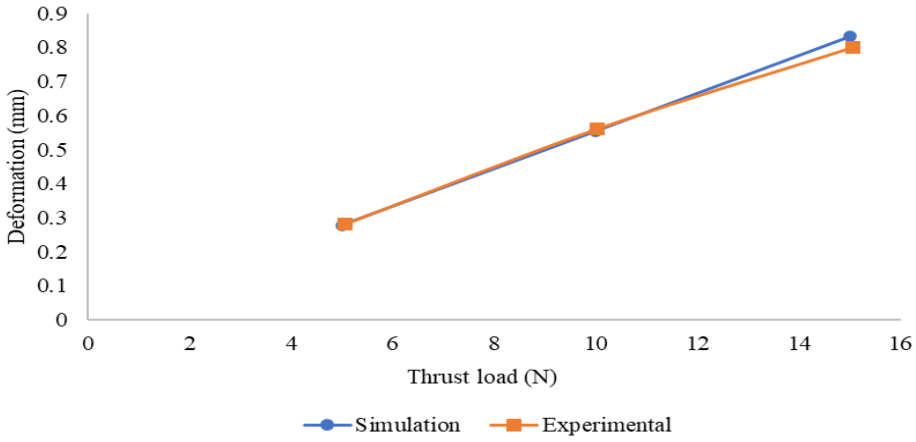

Figure 12. Comparison between simulation and experimental deformation under thrust load

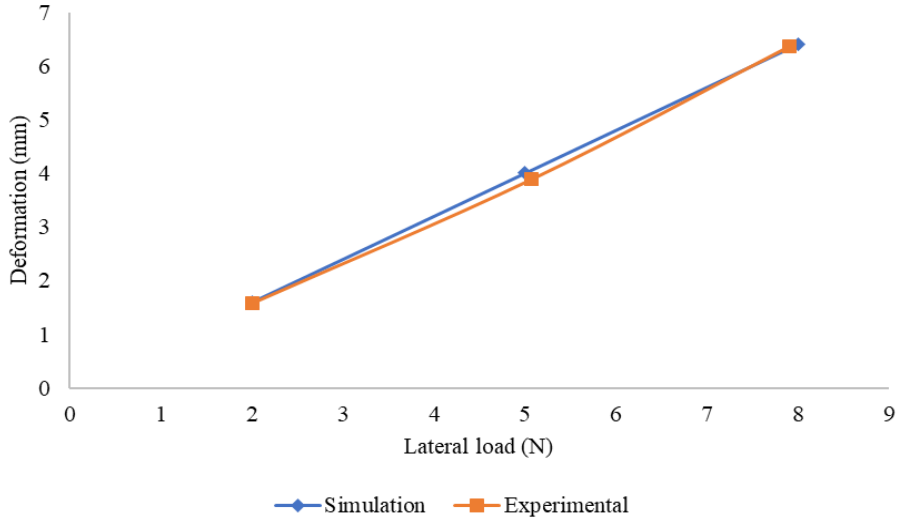

Figure 13. Comparison between simulation and experimental deformation under lateral load

Figures 12 and 13 show that both simulation and experimental curves follow nearly identical linear trends for thrust and lateral loading. This consistency demonstrates that the optimized structure behaves elastically and predictably within the tested load range. Although deformation under lateral loading was higher than under thrust loading, the correlation between simulation and experimental results remained strong. Minor deviations may be attributed to practical factors such as slight misalignment during load application, dimensional tolerances from the 3D printing process, and the anisotropic characteristics of PLA produced through fused filament fabrication. These factors can introduce small variations in stiffness that are not fully captured in the numerical model.

The strong correlation between simulation and experimental results validates the effectiveness of the topology optimization and finite element analysis approach used in this study. It also confirms that the optimized drone arm maintains structural integrity and predictable mechanical performance under both dominant thrust loads and secondary lateral loads encountered during typical UAV operation.

The flight performance of the drone was evaluated by comparing the energy consumption of the original arm design and the optimized arm (Design 2.0) during hovering flight. The evaluation focused on battery usage as an indicator of propulsion efficiency and overall energy demand. Each configuration was tested through a 5-minute indoor hovering flight under stable manual control to minimize external disturbances. Three repeated trials were conducted for each configuration to ensure consistency of the results.

The measured parameters included the final voltage of each cell in the 3S Li-Po battery after flight and the recharge capacity required to restore the battery to full charge. The recharge capacity (mAh) recorded by the

https://doi.org/10.29303/dtm.v16i1.1218

Li-Po charger represents the amount of electrical energy consumed during the flight. The results of these measurements are summarized in Table 8.

Table 8. Battery voltage and recharge data

Design	Data	Cell 1 (V)	Cell 2 (V)	Cell 3 (V)	Total Voltage(V)	Recharge (mAh)
Original	1	3.68	3.69	3.70	11.07	1429
	2	3.69	3.69	3.70	11.08	1413
	3	3.69	3.70	3.71	11.10	1417
2.0	1	3.75	3.76	3.76	11.27	1209
	2	3.75	3.76	3.76	11.27	1217
	3	3.74	3.75	3.76	11.25	1224

The experimental results show that Design 2.0 consumed an average of 1216.7 mAh, whereas the original design required an average of 1419.7 mAh for the same hovering duration. This represents a reduction of approximately 203 mAh, or 14.3% lower energy consumption, when using the topology-optimized arm. In addition, the final battery voltage of Design 2.0 remained slightly higher after each flight compared to the original configuration, indicating reduced discharge levels and lower power demand during operation.

Assuming a proportional relationship between battery consumption and flight duration, the 14.3% reduction in energy usage corresponds to an estimated hovering time increase of approximately 50 seconds under the same battery capacity and operating conditions. This improvement demonstrates that topology optimization not only enhances structural efficiency but also contributes to improved operational endurance. Overall, the flight test results confirm that the implementation of topology optimization on the drone arm successfully reduces energy consumption while maintaining stable flight performance and structural integrity.

4. CONCLUSION

This study presented an integrated approach combining topology optimization, finite element analysis, additive manufacturing, and experimental validation for improving the structural and operational performance of a DJI F450 drone arm. The topology optimization process successfully removed non-critical material while preserving key load-bearing regions, resulting in a structurally efficient and lightweight configuration.

The novelty of this study lies in the comprehensive validation of a topology-optimized drone arm through both mechanical testing and real flight performance evaluation. Unlike previous studies that primarily focused on structural simulation or frame-level optimization, this research demonstrates the direct relationship between component-level topology optimization, structural behavior, and UAV energy efficiency through experimental verification and flight testing.

The optimized arm achieved a 53.1% mass reduction while maintaining safety factors above acceptable limits. Simulation and experimental validation showed strong agreement, with deformation deviations ranging from 0.64% to 3.89%, confirming the reliability of the numerical model. Furthermore, flight performance evaluation revealed that the reduced structural mass decreased battery consumption by approximately 14.3% and extended hovering time by about 50 seconds.

These results confirm that the integration of topology optimization and additive manufacturing can produce lightweight, structurally reliable, and energy-efficient UAV components. The study provides a practical scientific and engineering contribution by demonstrating that component-level structural optimization can simultaneously improve mechanical performance and operational endurance, offering a validated design strategy for future UAV development.

ACKNOWLEDGMENTS

This research was fully funded by Udayana University through the Institute of Research and Community Service. The authors would also like to thank the *Studio Perancangan dan Rekayasa Sistem* (SPRS) Laboratory, Department of Mechanical Engineering, Brawijaya University, for the ANSYS research facilities.

REFERENCES

Abeywickrama, H.V., Jayawickrama, B.A., He, Y., Dutkiewicz, E, Comprehensive energy consumption model for unmanned aerial vehicles based on empirical studies of battery performance, IEEE Access, 6, 58383–58394, 2018.

Al-Haddad, L.A., Quadcopter unmanned aerial vehicle structural design using an integrated approach of topology optimization and additive manufacturing, Designs (Basel), (8)58, 2024. https://doi.org/10.3390/designs8030058

Aravind S. (n.d.). F450 FRAME [3D model], 2019. https://grabcad.com/library/f450-frame-1

Asif, S. H., Hasan, K., Dhar, N.R., Topology optimization and 3D printing of a unibody quadcopter airframe, IOP Conference Series: Materials Science and Engineering, 1305(1), 012021, 2024.

Bay, B., Eryıldız, M., Design and analysis of a topology-optimized quadcopter drone frame, Gazi Üniversitesi Fen Bilimleri Dergisi Part C: Tasarım ve Teknoloji, 12(2), 427–437, 2024.

Bright, J., Suryaprakash, R., Akash, S., Giridharan, A., Optimization of quadcopter frame using generative design and comparison with DJI F450 drone frame, IOP Conference Series: Materials Science and Engineering, 1012(1), 2021.

Darsin, M., Advanced optimization of drone frame design through the application of generative design techniques and 3D printing technology, Journal of Mechanical Science and Technology, 39(1), 119–128, 2025.

Hanon, M. M., Marczis, R., Zsidai, L, Influence of the 3D printing process settings on tensile strength of PLA and HT-PLA, Periodica Polytechnica Mechanical Engineering, 65(1), 38–46, 2021.

Hossain, R., A , Short review of the drone technology, International Journal of Mechatronics and Manufacturing Technology, 7(2), 2022.

Karohika, I.M.G., Haruyama, S, The real contact width evaluation of a three-layer metal gasket, SINERGI, 26(3), 2022.

Ngo, T.D., Kashani, A., Imbalzano, G., Nguyen, K.T.Q., Hui, D, Additive manufacturing (3D printing): A review of materials, methods, applications and challenges, Composites Part B: Engineering, 143, 172-196, 2018. https://doi.org/10.1016/j.compositesb.2018.02.012

Pöcher, P.K., Drone design and construction for indoor inspection scenarios, Master's thesis, Norwegian University of Science and Technology, Trondheim, Norway, 2018.

Shu, J., Luo, H., Zhang, Y., Liu, Z, 3D printing experimental validation of the finite element analysis of the maxillofacial model, Frontiers in Bioengineering and Biotechnology, 9, 1-7, 2021. https://doi.org/10.3389/fbioe.2021.694140

Soon, C. F., Yee, S. K., Nordin, A. N., Rahim, R. A., Ma, N. L., Hamed, I. S. L. A., Tee, K. S., Azmi, N. H., Sunar, N. M., Heng, C, Advancements in biodegradable printed circuit boards: review of material properties, Fabrication Methods, Applications and Challenges. International Journal of Precision Engineering and Manufacturing 25(9), 1925–1954, 2024.

Thibbotuwawa, A., Nielsen, P., Zbigniew, B., Bocewicz, G, Energy consumption in unmanned aerial vehicles: A review of energy consumption models and their relation to UAV routing, Advances in Intelligent Systems and Computing, Springer, 853, 173–184, 2019. https://doi.org/10.1007/978-3-319-99996-8_16

Ultimaker, Ultimaker-PLA-TDS-v5.00, Retrieved June 20, 2025, 2022. https://um-support-files.ultimaker.com/materials/2.85mm/tds/PLA/Ultimaker-PLA-TDS-v5.00.pdf.

Winangun, K., Lostari, A., Riani, N.I., Pemodelan mesin diesel dual fuel (DDF) menggunakan bahan bakar biodiesel dan gas hidrogen, Turbo: Jurnal Program Studi Teknik Mesin, 13(2), 2024.

Zadravec, M., Kramberger, J., Nečemer, B., Glodež, S, Fatigue behaviour of PA66 GF30 at different temperatures, Polymers (Basel), 17(1), 2025.

Zhu., Li, Light-weighting in aerospace component and system design, Propulsion and Power Research, 7(2), 103-119, 2018. https://doi.org/10.1016/j.jppr.2018.04.001